ELSEVIER

Antiviral Research 56 (2002) 99–114

Antiviral Research

www.elsevier.com/locate/antiviral

Biochemical characterization of rhinovirus RNA-dependent RNA polymerase

Magdeleine Hung, Craig S. Gibbs, Manuel Tsiang *

Gilead Sciences, 333 Lakeside Drive, Foster City, CA 94404, USA

Received 14 March 2002; accepted 13 June 2002

Abstract

Human rhinoviruses (HRV) represent the single most important causative agent of the common cold. The HRV genome encodes an RNA-dependent RNA polymerase (RdRp) designated 3D polymerase that is required for replication of the HRV RNA genome. We have expressed and purified recombinant HRV-16 3D polymerase to near homogeneity from *Escherichia coli* transformed with an expression plasmid containing the full-length 460 amino acid HRV-16 3D sequence with a methionine at the N-terminus and a glycine–serine linker followed by a 6-histidine affinity tag at the C-terminus. The purified recombinant protein has rifampicin-resistant activity in a poly(A)-dependent poly(U) polymerase assay while corresponding fractions similarly purified from *E. coli* transformed with an expression plasmid without the HRV-16 3D sequence showed no activity. The optimal conditions for temperature, pH, divalent cations Mg^{2+} and Mn^{2+}, and KCl were determined. The recombinant protein has RNA polymerase activity on homopolymeric templates poly(A) and poly(C) and heteropolymeric RNA templates primed with either RNA or DNA oligonucleotide primers or self-primed by a copy-back mechanism. A unique, secondary structureless heteropolymeric RNA template that is an efficient substrate was developed to facilitate kinetic characterizations of the enzyme. In the presence of Mg^{2+}, the enzyme displayed strong base and sugar specificity. However, when Mg^{2+} was replaced by Mn^{2+} specificity for ribonucleotides was lost, utilization of deoxynucleotides became possible and primer-independent activity was observed on the poly(C) template. Zn^{2+} was found to inhibit HRV-16 3D polymerase with an IC_{50} as low as 0.6 μM by a mechanism distinct from the magnesium ion stimulation. The activity of this 6His-tagged HRV-16 3D polymerase was compared with that of a recombinant HRV-16 3D polymerase expressed without the 6His-tag and was found to be identical. The availability of recombinant rhinovirus RdRp in a purified form will facilitate the structure–function analysis of this enzyme as well as the identification of specific inhibitors to the rhinovirus 3D polymerase that have therapeutic value in the treatment of the common cold.

Keywords: Rhinovirus; Polymerase; Inhibition; Screening; Zinc

1. Introduction

Human rhinovirus (HRV) is the major etiologic agent causing more than 50% of common colds (Pitkaranta and Hayden, 1998). The rhinoviruses

* Corresponding author. Tel.: +1-650-522-5860; fax: +1-650-522-5890

E-mail address: manuel_tsiang@gilead.com (M. Tsiang).

0166-3542/02/$ - see front matter
PII: S0166-3542(02)00101-8

constitute the largest genus of the picornavirus family of non-enveloped positive strand RNA viruses. This family also includes the enteroviruses of which poliovirus is the best characterized member (Palmenberg, 1990; Richards and Ehrenfeld, 1990; Porter, 1993). Rhinovirus and poliovirus are very similar in genome organization, polyprotein structure and processing, and viral protein function (Racaniello and Baltimore, 1981; Stanway et al., 1984). Over 100 distinct serotypes of rhinoviruses have been identified. Ninety percent of these serotypes utilize ICAM-1 as a receptor for infecting HeLa cells and are thus referred to as the 'major' receptor group (Tomassini and Colonno, 1986; Greve et al., 1989). All the remaining rhinovirus serotypes, with one exception, utilize the LDL receptor (Hofer et al., 1994) and are referred to as the 'minor' receptor group. To date, the complete genome sequence of only five HRV serotypes (serotypes 14, 16 and 89 from the 'major' group and serotypes 1B and 2 from the 'minor' group) has been determined (Stanway et al., 1984; Skern et al., 1985; Duechler et al., 1987; Hughes et al., 1988; Lee et al., 1994).

Due to the numerous antigenic types of HRVs, vaccine development has been hampered as a viable approach for the prevention of rhinoviral infections. Instead, non-structural proteins that are both necessary for viral replication and highly conserved within the picornarviridae family, such as the 3C protease, have become attractive targets for antiviral development (Patick and Potts, 1998; Wang, 1999). Among these targets is the rhinoviral 3D polymerase encoded at the C-terminal portion of the polyprotein (Gwaltney and Rueckert, 1997). To date, poliovirus 3D polymerase remains the most extensively characterized picornaviral polymerase, both as purified preparations from poliovirus infected HeLa cells (Van Dyke and Flanegan, 1980; Young et al., 1985; Andrews et al., 1985; Lubinski et al., 1987) and as purified recombinant proteins expressed in *Escherichia coli* and insect cells (Morrow et al., 1987; Richards et al., 1987; Rothstein et al., 1988; Plotch et al., 1989; Neufeld et al., 1991a,b; Gohara et al., 1999). The poliovirus 3D polymerase is an RNA-dependent RNA polymerase (RdRp) (Kuhn and Wimmer, 1987; Semler et al., 1988; Richards and Ehrenfeld, 1990). As this class of polymerases is unique to RNA viruses and has no host counterpart, the viral RdRp represents a very attractive target for antiviral design. Comparison of the amino acid sequences identified several motifs in poliovirus 3D polymerase that are conserved among other RdRps (Poch et al., 1989; Koonin, 1991; Bruenn, 1991), suggesting shared catalytic functions. More recently, the crystal structure of poliovirus 3D polymerase has been determined as a first example of a structure of a RdRp (Hansen et al., 1997). With greater than 50% identity at the amino acid level to the poliovirus 3D polymerase, the rhinovirus 3D polymerase is expected to have very similar properties. Although a rhinoviral polymerase activity has been purified from rhinovirus 2 infected HeLa cells 16 years ago (Morrow et al., 1985), characterization of a recombinant 3D polymerase from HRV-2, a member of the minor receptor group has only been reported recently (Gerber et al., 2001).

In this study, we report the purification and biochemical characterization of mature rhinovirus 3D polymerase from serotype 16 (Genbank accession # NC_001752) as a 6His-tagged protein expressed in *E. coli*. Of the two best characterized serotypes of the 'major' receptor group, HRV-14 and HRV-16, we have chosen to study the 3D polymerase from HRV-16 because amino acid sequence comparison indicates that HRV-16 has significantly higher homology than HRV-14 to the other HRV of both receptor groups whose full genome sequence is known and is, therefore, a better overall representative of HRV (Lee et al., 1994). Moreover, the crystal structure of HRV-16 virion has been determined (Oliveira et al., 1993), the virus causes measurable cytopathic effects in tissue culture with a 20-fold lower $TCID_{50}$ than HRV-14 (Couch, 1990), and causes cold symptoms following experimental infection of susceptible human volunteers (Bush et al., 1978; Lemanske et al., 1989; Calhoun et al., 1991). Thus, HRV-16 is a strain that has been highly characterized at the molecular, cellular and clinical levels.

2. Materials and methods

2.1. Construction of recombinant plasmids

HRV-16 viral RNA was extracted from 100 μl of HRV-16 (ATCC #VR-283) containing tissue culture medium from infected HeLa cells obtained from ATCC using the QIAamp Viral RNA Kit (QIAGEN, Valencia, CA). cDNA was generated using the Advantage® RT-PCR Kit (Clonetech, Palo Alto, CA). The coding region of HRV-16 3D polymerase was PCR-amplified using two primers containing HRV-16 sequence and cloning sites, XhoI/NdeI/HRV 5′primer: 5′GACTATCTCGAGCATATGGGCCAAATT CAAATCT3′ and HRV/GS/6His/KpnI 3′primer: 5′ATAGTCGGTACCTCAATGGTGATGGTG ATGGTGAGAACCGAATTTTTCATACCATT CATGTCT3′. The amplified product encodes an additional initiator methionine at the N-terminus of the 3D polymerase (Gly^{1694} in polyprotein) and a 6His affinity tag preceded by a glycine–serine linker at the C-terminus (Phe^{2153} in polyprotein). The PCR product was digested with NdeI and KpnI and subcloned directly into the expression vector pRSETB (InVitrogen, Carlsbad, CA) to give pHRV16-3D6His. The sequence of the clone was confirmed by dideoxy sequencing to be identical to the published HRV-16 3D sequence (Lee et al., 1994). For construction of the native HRV-16 3D polymerase, the GS-6His sequence from pHRV16-3D6His was deleted by replacing the 344 bp C-terminal fragment between the PstI site in the polymerase coding region and the KpnI site in the vector with the corresponding 320 bp fragment obtained by PCR amplification using a 3′primer without the GS-6His sequence. Sequence of the new construct, pHRV16-3D was confirmed by dideoxy sequencing.

2.2. Expression and purification of HRV-16 RNA polymerase

E. coli, BL21(DE3) pLysS (Stratagene, La Jolla, CA) was transformed with pHRV16-3D6His for protein expression. The culture was grown at 37 °C to an OD of 0.8–1.0 and expression was induced overnight at 25 °C with the addition of 0.4 mM IPTG. Cells were harvested by centrifugation and the pellet was stored frozen at −80 °C. Five grams of cell pellet were resuspended in 30 ml of lysis buffer (50 mM Na Phosphate pH 7.5, 300 mM NaCl, 10% glycerol, 4 mM β-mercaptoethanol, 10 μg/ml DNAse I, 20 μg/ml RNase A, 500 μg/ml lysozyme) and sonicated on ice for 1.5 min. The lysate was mixed for an hour at 4 °C to facilitate extraction of proteins. The lysate was centrifuged at 43 000 × *g* for 1 h in a Sorvall SS-34 rotor. The supernatant was collected and adjusted to 20 mM imidazole by adding an equal volume of adjustment buffer (75 mM Na Phosphate pH 7.5, 300 mM NaCl, 10% glycerol, 40 mM imidazole) before chromatography on a Ni-NTA column (QIAGEN). Proteins were eluted with an imidazole gradient of slope = 3.2 mM/ml in column buffer (50 mM NaPhosphate pH 7.5, 300 mM NaCl, 10% glycerol, 20 mM imidazole) from 20 to 500 mM imidazole. Eluted fractions were analyzed on 10% SDS polyacrylamide gels and the protein bands were stained with the NOVEX Colloidal Blue Staining Kit (InVitrogen). To remove the imidazole, the pooled fractions containing the HRV-16 3D6His protein were dialyzed twice against 1000 ml of dialysis buffer (50 mM NaPhosphate pH 7.5, 150 mM NaCl, 10% glycerol), once against 250 ml of the same buffer containing 50% glycerol at 4 °C, aliquoted and stored at −80 °C. The protein concentration was determined using the Micro BCA Protein Assay Reagent (Pierce, Rockford, IL).

2.3. Enzymatic assays

The poly(A)-dependent, oligo(U)-primed polymerase assay was performed as previously described (Neufeld et al., 1991a) with the following modifications. The reaction was incubated at 30 °C for 30 min in a final volume of 30 μl in the optimized buffer (50 mM Tris-HCl pH 7.0, 1.5 mM $MgCl_2$, 10 mM KCl, 4 mM DTT and 20 Units of RNAsin). Unless otherwise specified, the reaction contained 20 nM purified HRV-16 3D, 16 ng/μl of poly(A) and 160 nM oligo$(U)_{15}$, 10 μCi of [α-^{33}P]-UTP (NEN, ~3000 Ci/mmol) and 11 μM UTP. Primer and template were pre-annealed by incubation at 95 °C for 5 min followed by 37 °C

for 5 min before addition to the reaction. Incorporation of [α-^{33}P]-UMP into RNA was determined by spotting 9 μl of the reaction on Whatman 3 MM filter disk (catalog #1030025). The filter was then washed three times in a solution containing 5% trichloroacetic acid (TCA) and 20 mM sodium pyrophosphate and once in 95% ethanol. The air-dried filter was counted in scintillation fluid.

When a biotinylated DNA primer was used, the reaction was terminated by adding 9 μl of the reaction to 45 μl of 17 mM EDTA in PBS (150 mM NaCl, 1.5 mM NaH_2PO_4, 8.5 mM K_2HPO_4) in a well of a Streptavidin FlashPlate®Plus (NEN, Boston, MA). The incorporated label was captured through the biotin–streptavidin interaction and quantified by using a TopCount.NXT™ (Packard Instrument, Meriden, CT). When heteropolymeric templates were used, the reaction contained 8 ng/μl of RNA template with or without 160 nM biotinlylated DNA primers, 10 μCi of a single [α-^{33}P]-labeled NTP ([α-^{33}P]ATP, [α-^{33}P]UTP, [α-^{33}P]GTP, or [α-^{33}P]CTP) and 500 μM each of the remaining three NTPs. The labeled nucleotide was used at a concentration equal to the Michaelis constant (K_m) of the nucleotide (see Table 3).

2.4. Heteropolymeric hairpin template

A self-priming heteropolymeric hairpin RNA was cloned into the pGEM-3Zf(+) vector and transcribed using the RiboMAX™ large scale RNA production system-T7 (Promega, Madison, WI). The hairpin RNA was an RNA of 309 nucleotides starting with the vector sequence (5′GGGCG3′) followed by 248 nucleotides of HBV sequence (nucleotides 1408–1655 of HBV genome, Genbank accession # X02763) with a 23 bp stem-loop structure (5′ AGCTTGCATGCCTGCAGGTCGACAAAATCTAGAGTCGACCTGCAGGCATGCAAGCT 3′) engineered at the 3′end of the RNA.

2.5. Contruction of a secondary structureless heteropolymeric RNA template

A 244 nucleotide secondary structureless heteropolymeric RNA (sshRNA) of the following sequence: $(TCAG)_{20}(TCCAAG)_{14}(TCAG)_{20}$ was assembled by PCR using DNA oligonucleotides containing those repetitive sequences as templates. The assembled PCR product containing those 244 nucleotides was cloned into the pGEM-3Zf(+) vector (Promega) under the control of the T7 polymerase promoter. Dideoxy sequencing confirmed the sequence of the sshRNA insert in the clone selected for in vitro transcription. The sshRNA transcripts were synthesized using the RiboMAX™ large scale RNA production system-T7 (Promega). The sequence of the sshRNA was verified to be devoid of secondary structures by the RNA-folding algorithm, RNAstructure 3.5 developed by Mathews et al. (1999). In the polymerase assay using the sshRNA, an equimolar mixture of four primers whose sequences are shown as follows was used:

C1 primer 3′AGTCAGTCAGTCAGT*GT*-biotin 5′,
A1 primer 3′GTCAGTCAGTCAGTC*TC*-biotin 5′,
G1 primer 3′TCAGTCAGTCAGTCA*CA*-biotin 5′,
T1 primer 3′CAGTCAGTCAGTCAG*AG*-biotin 5′.

Each primer, when annealed to the sshRNA will allow RNA synthesis to start with a different base to allow unbiased incorporation of all four nucleotides.

2.6. Gel analysis of polymerase reaction products

Polymerase assays were run for 1 h. The reaction was stopped by the addition of an equal volume of 2X Proteinase K buffer (300 mM NaCl, 100 mM Tris–HCl, pH 7.5 and 1% SDS) and 50 μg proteinase K. Proteinase digestion was done at 37 °C for 30 min in the presence of 20 μg yeast tRNA carrier. The RNA was extracted once with phenol/chloroform and precipitated with equal

volume of isopropanol. The RNA pellet was resuspended in formamide loading buffer and separated by electrophoresis on either a 5% or a 13.5% denaturing (8 M urea) polyarylamide gel. Gels were run at 0.03 W/cm^2 for 1.5 h and dried before autoradiography.

3. Results

3.1. Expression of rhinovirus 3D polymerase in E. coli

To conduct biochemical characterization of rhinovirus RdRp, the 3D polymerase-encoding cDNA from HRV-16 was PCR amplified and cloned under the control of a T7 RNA polymerase promoter. Overnight induction of the *E. coli* harboring pHRV16-3D6His at 25 °C resulted in high-level expression of a 54 kDa protein in the soluble fraction of the bacterial lysate (Fig. 1A, lane 3). This 54 kDa protein was absent in the corresponding fraction obtained from the *E. coli* transformed with the expression vector alone (Fig. 1A, lane 2). This 54 kDa protein was purified from the soluble fraction of the lysate from a 2000 ml culture (i.e. ~10 g of cell pellet) using a single Ni-NTA column. The majority of the 54 kDa protein bound to the Ni-NTA resin as it disappeared from the flow-through fraction (Fig. 1B, lane 2). After washing the column extensively with column buffer, the 54 kDa protein peak eluted from the column at a concentration of imidazole between 58 and 134 mM (Fig. 1B, lanes 5–11). The fractions (58–134 mM imidazole) containing the 54 kDa band were pooled, dialyzed and used for polymerase activity assays. The purified protein had an estimated purity of >95% based on silver-stained SDS-PAGE and the yield was ~61 mg/l of *E. coli* culture.

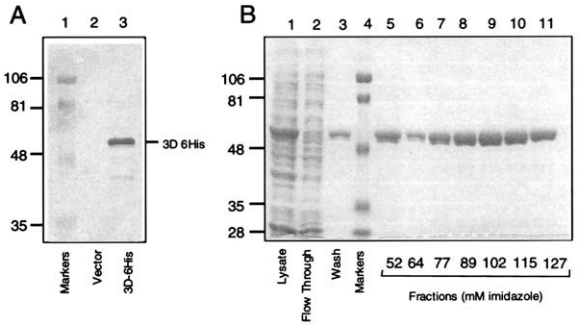

Fig. 1. Expression and purification of HRV16 3D polymerase. (A) Western blot probed with anti-6His antibody of soluble cell extract from *E. coli* transformed with the empty vector (lane 2), and from *E. coli* transformed with pHRV16-3D6His (lane 3). Lane 1 contains prestained M.W. markers. (B) Purification steps and imidazole elution profile of HRV16 3D expressed in *E. coli*. The various fractions were run on a 10% SDS polyacrylamide gel and stained with the NOVEX Colloidal Blue. The imidazole concentration at which each fraction was eluted is indicated on the figure. The visible band intensity difference in lane 6 is probably due to a loading artifact.

3.2. RNA synthesis by 6His-tagged HRV-16 3D polymerase

The activity of HRV-16 3D-6His polymerase was first examined by the incorporation of [α-^{33}P]UMP using poly(A) and oligo(U)$_{15}$ as the template–primer pair. Incorporation of radioactivity was linearly dependent on the amount of enzyme (Fig. 2A). This RNA polymerase activity was not attributable to a co-purifying impurity since no radioactive incorporation was detected using the corresponding pooled fractions from a similar purification of the lysate of *E. coli* transformed by the vector alone (Fig. 2A). The activity of HRV-16 3D-6His polymerase was resistant to 20 μg/ml rifampicin, an inhibitor of *E. coli* DNA-dependent RNA polymerase (Chamberlin et al., 1983), while purified *E. coli* DNA-dependent RNA polymerase (Amersham Pharmacia Biotech, Piscataway, NJ) was almost completely inhibited by 20 μg/ml rifampicin irrespective of the reaction buffer used, providing further evidence that the observed activity is associated with the recombinant viral enzyme (Fig. 2B). The incorporation of labeled UMP was linear over 30 min (data not shown).

3.3. HRV-16 3D polymerase activity on homopolymeric templates

The recombinant HRV-16 polymerase was further tested for its ability to utilize different homopolymeric RNAs as templates and for the

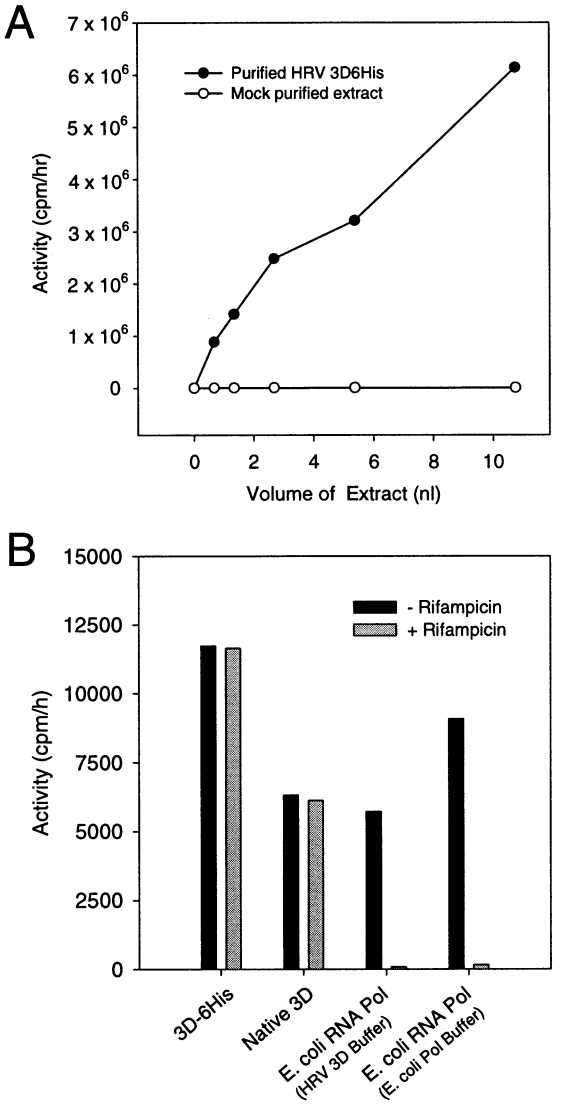

Fig. 2. (A) Linear dependence of the rate of nucleotide incorporation on the concentration of HRV16 3D polymerase. For the purified recombinant 3D6His polymerase, 10.75 nl of extract correspond to a final enzyme concentration of 60 nM in the reaction. Sampling of the desired amount of extract was achieved by serial dilution. (B) Resistance of HRV16 3D polymerase to rifampicin. Both 3D6His and native 3D were used at a final concentration of 5.3 pg/μl in the optimized HRV 3D buffer. *E. coli* polymerase was tested at a final concentration of 13 ng/μl in either the optimized HRV 3D buffer or in the *E. coli* polymerase buffer (40 mM Tris-HCl pH 7.5, 150 mM KCl, 10 mM $MgCl_2$, 0.01% Triton X-100). Rifampicin was used at a final concentration of 20 μg/ml.

efficiency of oligoRNA and oligoDNA to serve as primers. The incorporation of ^{33}P-ribonucleotides into TCA-precipitable products was determined either in the presence of 1.5 mM Mg^{2+} or Mn^{2+} (Table 1).

In the presence of Mg^{2+}, significant activity was observed when poly(A) or poly(C) was used as templates and the activity was template and primer-dependent. In contrast, poly(G) and poly(U) templates were not efficient substrates. Biotinylated oligoDNA primers appeared to work slightly more efficiently than oligoRNA primers. The ability of the recombinant HRV-16 polymerase to utilize biotinylated DNA primers allowed the reactions to be performed in NEN Flash Plates for subsequent analyses.

In the presence of Mn^{2+}, the overall activity of all reactions was stimulated by 2.5–5.6-fold with the same template and primer specificity. However, RNA synthesis using poly(C) as template became primer-independent, suggesting de novo initiation of template-directed RNA synthesis or terminal transferase activity (Table 1). This primer-independent activity is clearly distinct from the activity seen with poly(C) in primed syntheses, where the Mn^{2+} stimulation relative to Mg^{2+} was only 2.7–4.3-fold.

3.4. Optimization of the HRV-16 polymerase reaction conditions

The reaction conditions for the HRV-16 3D-6His polymerase were optimized using poly(A) as the template and biotinylated oligo$(dU)_{15}$ as the primer in NEN Flash Plates (Fig. 3). The incubation temperature was varied between 12 and 37 °C, and the optimum temperature was approximately 30 °C (Fig. 3A). At temperatures between 32 and 37 °C, there was a dramatic decrease in activity.

Using the optimum temperature of 30 °C, the pH dependence of RdRp activity displayed a bell-shaped curve with a pH optimum of 7.3 (Fig. 3B).

Divalent metal ions were absolutely required for activity and the optimum concentration for Mg^{2+} was 1 mM (Fig. 3C). Mn^{2+} was able to substitute for Mg^{2+} while stimulating the activity by ~2.5-fold at the optimum concentration of 1 mM (Fig.

Table 1
HRV-16 3D polymerase activity on homopolymeric templates

Template	Primer[a]	Incorporation[b] (10^3 cpm/h)		
		Mg^{2+}	Mn^{2+}	(Mn^{2+}/Mg^{2+})
Poly(A)	No primer	3	5	
	$(U)_{15}$	2393	5981	(2.5)
	Biotin-$(dC)_2(dT)_{15}$	4307	13 060	(3.0)
Poly(C)	No primer	3	10 108	(3300)
	$(G)_{15}$	277	1188	(4.3)
	Biotin-$(dA)_2(dG)_{15}$	1839	5026	(2.7)
Poly(G)	No primer	3	7	
	$(C)_{15}$	2	10	(5.0)
	Biotin-$(dT)_2(dC)_{15}$	2	5	(2.5)
Poly(U)	No primer	2	3	
	$(A)_{15}$	5	28	(5.6)
	Biotin-$(dG)_2(dA)_{15}$	4	14	(3.5)

[a] Each reaction contains 4.8 pmol of primer annealed to 0.48 μg of template.
[b] Radioactive incorporation was quantitated by TCA precipitation of 9 μl of reaction on Whatman 3 mm paper discs. Mg^{2+} and Mn^{2+} were each used at 1.5 mM.

3C). However, the polymerase activity dropped sharply at 3 mM Mn^{2+}. At low concentrations (< 10 mM), the monovalent cation K^+ exhibited a modest stimulatory effect but became inhibitory at higher concentrations with optimum activity observed at 10 mM (Fig. 3D).

3.5. Substrate specificity of HRV-16 3D polymerase

We studied the substrate specificity of HRV-16 3D polymerase in the presence of either 1.5 mM Mg^{2+} or Mn^{2+} by testing the ability of the enzyme to incorporate different nucleotides into nucleic acid products. Using the poly(A)/oligo$(dT)_{15}$ template–primer pair, we measured radioactive incorporation of [α-^{33}P]-labeled GTP, ATP, CTP, UTP and dTTP. As shown in Table 2, HRV-16 polymerase misincorporates non-complementary ribonucleotides with very low efficiency. This base specificity was not sensitive to substitution of Mg^{2+} by Mn^{2+}. In the presence of Mg^{2+}, the enzyme could not polymerize dTMP, suggesting that the enzyme was devoid of significant reverse transcriptase activity. However, when [α-^{33}P]-labeled dTTP was mixed with unlabeled UTP at a molar ratio of 1:100, there was a low level of misincorporation of labeled dTMP into the RNA, suggesting that an occasional deoxyribose may be tolerated if the enzyme is not compelled to incorporate more than one dTMPs in a row. When Mg^{2+} was replaced by Mn^{2+}, sugar specificity was compromised, reverse transcriptase activity was stimulated by 800-fold and misincorporation of dTMP during active RNA polymerization was increased by 1200-fold.

3.6. HRV-16 3D polymerase activity on heteropolymeric templates

An ideal RNA template for high throughput screening using the RNA polymerase assay should (1) allow for unbiased incorporation of all four NTPs; (2) contain repetitive sequences to allow multiple priming, as occurs with homopolymeric templates, in order to maximize the signal; and (3) be devoid of any secondary structure that could contribute to preferential self-priming and copy-back which competes with priming by biotinylated primers necessary for signal detection using the Flash Plate method. To meet these criteria, a secondary structureless heteropolymeric RNA (sshRNA) template was designed (see materials and methods) and compared with the homopolymeric templates poly(A) and poly(C), and the self-priming heteropolymeric hairpin RNA template

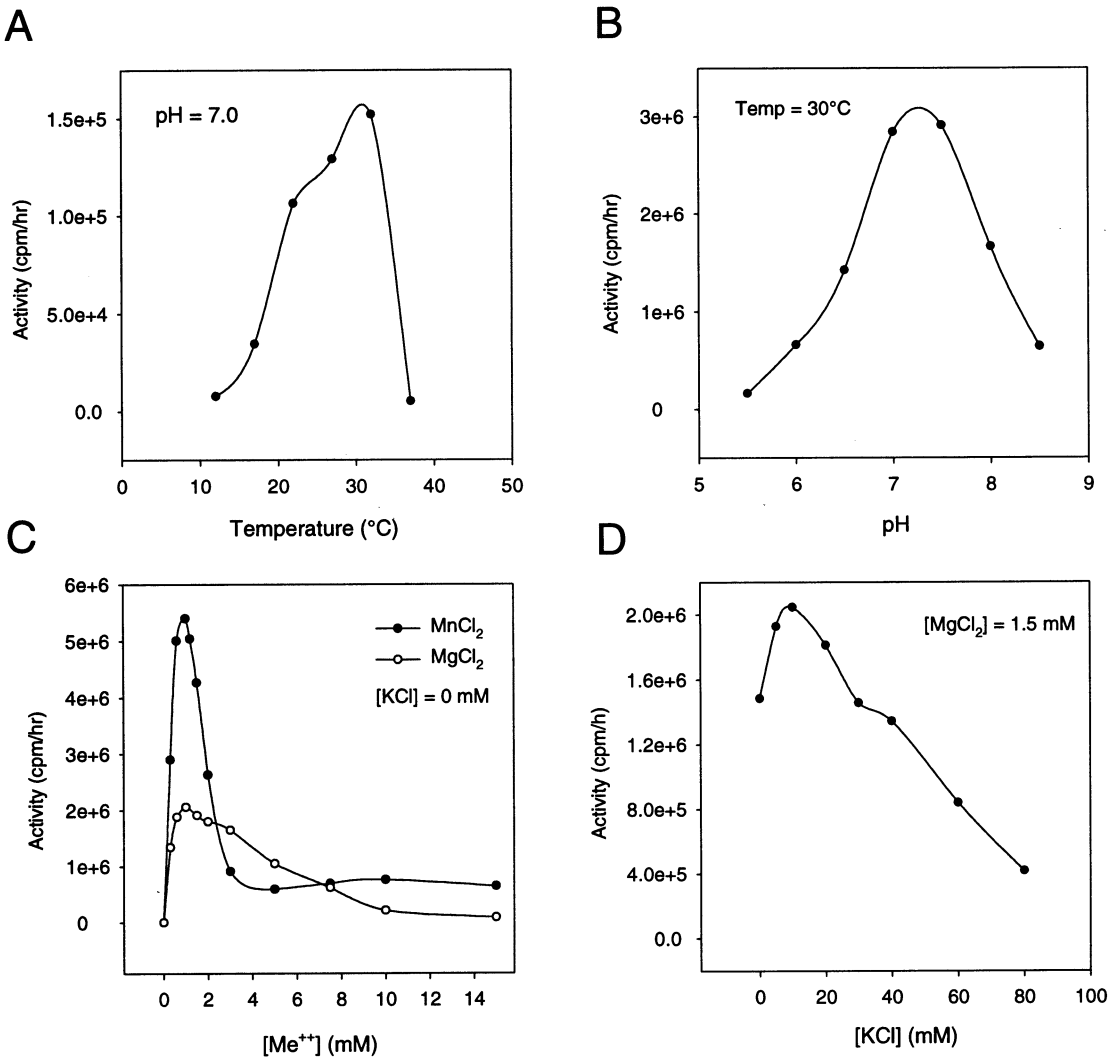

Fig. 3. Optimization of the reaction conditions for HRV16 3D polymerase. (A) pH optimization. (B) Temperature optimization. (C) Divalent cation optimization. (D) KCl optimization.

using the same labeling conditions. The homopolymeric templates, poly(A) and poly(C) directed divergent levels of incorporation of UTP and GTP into TCA precipitable material (Fig. 4A). In contrast, the sshRNA template and the self-primed heteropolymeric hairpin RNA template directed incorporation of UTP and GTP at comparable rates (Fig. 4A). Among the heteropolymeric RNA templates, sshRNA was a more efficient substrate by 3–4-fold than the hairpin RNA (Fig. 4A). However, when sequence specific biotinylated primers were used on hairpin RNA, and the signal captured on the Flash Plate, the signal for hairpin RNA became dramatically lower than the signal for sshRNA (Fig. 4B), suggesting that oligonucleotide priming in trans is much less efficient than self-priming on the hairpin RNA templates.

To further characterize the activity of HRV-16 3D polymerase, the reaction products of sshRNA and hairpin RNA templates were analyzed by gel electrophoresis (Fig. 4C). When sshRNA template was used, RNA molecules over a range of sizes

Table 2
Substrate specificity of HRV16 3D polymerase*

Labeled NTP (0.11 μM)[a]	Unlabeled NTP (11 μM)[a]	Incorporation[b] (10^3 cpm/h)		
		Mg^{2+}	Mn^{2+}	(Mn^{2+}/Mg^{2+})
[α-^{33}P]-GTP	GTP	1.0	0.9	(1)
[α-^{33}P]-ATP	ATP	0.1	0.1	(1)
[α-^{33}P]-CTP	CTP	0.2	2.7	(14)
[α-^{33}P]-UTP	UTP	3697	9075	(2.5)
[α-^{33}P]-dTTP	dTTP	0.2	169	(845)
[α-^{33}P]-dTTP	UTP	0.9	1138	(1264)

*, Each reaction contains 4.8 pmol of biotinylated $(dC)_2(dT)_{15}$ primer annealed to 0.48 μg of Poly(A) template.
[a] The final concentrations of labeled and unlabeled nucleotides in the reaction are indicated.
[b] Radioactive incorporation was quantitated by streptavidin capture on NEN Flash Plates. Mg^{2+} and Mn^{2+} were each used at 1.5 mM.

were synthesized by the recombinant enzyme as a result of multiple priming sites (Fig. 4C, lane 2). The longest product had a size similar to that of the input template (Fig. 4C, lane 1). The enzyme could also use the hairpin RNA templates to form a dimer-sized product as a result of self-priming (Fig. 4C, lanes 4). This dimer-sized product can form a long hairpin by intra-molecular base pairing and is thus very difficult to denature and will behave as a rod with a higher mobility than the monomer even in a denaturing gel electrophoresis (Behrens et al., 1996). For the hairpin RNA, a fraction of the dimer-sized product may be partially denatured and migrates as a smear at the top of the gel (Fig. 4C, lane 4).

3.7. Kinetic analysis of HRV-16 3D polymerase

To determine the K_m and k_{cat} for UTP and GTP, poly(A)/biotin$(dC)_2(dT)_{15}$ and poly(C)/biotin$(dA)_2(dG)_{15}$ template–primer pairs were used. Since HRV-16 3D could not utilize poly(G) and poly(U) as templates, determination of the K_m values for ATP and CTP on homopolymeric templates was not feasible. However, using the heteropolymeric template sshRNA, the K_m and k_{cat} values for all four ribonucleotide triphosphates could be determined using varying concentrations of a single radiolabeled nucleotide and saturating concentrations of the other three nonlabeled NTPs. The kinetic parameters obtained with both homopolymeric and sshRNA templates are summarized in Table 3. Using sshRNA as the template, UTP, GTP and ATP were incorporated with similar catalytic efficiencies. However, CTP was the most efficient substrate by a factor of 5–23-fold mainly due to a lower K_m relative to the other nucleotides. Using homopolymeric templates increased the catalytic efficiency of UTP and GTP incorporation mainly due to an increase in k_{cat}.

3.8. Inhibition of HRV-16 3D polymerase activity

In order to validate our 3D polymerase assay for the screening of inhibitors, we performed competition studies with increasing concentrations of one unlabeled NTP, dNTP or ddNTP, a fixed concentration of the corresponding limiting radiolabeled NTP and saturating concentrations of the three nonlabeled NTPs (Fig. 5). The IC_{50} values obtained for the unlabeled NTPs were consistent with their respective Michaelis constants (K_m), but the IC_{50} values for dNTPs and ddNTPs were 25–200-fold higher than those of the corresponding NTPs, further confirming that the recombinant 3D polymerase has a specificity for ribonucleotides over deoxyribonucleotides. We also tested the effects of gliotoxin, a non-nucleoside compound previously reported to inhibit viral RNA polymerases (Rodriguez and Carrasco, 1992; Ferrari et al., 1999). Gliotoxin inhibited HRV-16 3D polymerase with an IC_{50} of $\sim$150 μM (data not shown).

3.9. Inhibitory effect of Zn^{2+} ions

Because several previous studies reported the inclusion of 60 μM $ZnCl_2$ in the reaction buffers for poliovirus 3D polymerase (Plotch et al., 1989; Neufeld et al., 1991a; Gohara et al., 1999; Arnold and Cameron, 1999), we investigated the effect of Zn^{2+} on the activity of HRV-16 3D polymerase. Surprisingly, Zn^{2+} was inhibitory at 60 μM when tested in our standard HRV-16 3D assay buffer using PolyA/T as template. In Table 4, we have reported the IC_{50} values of Zn^{2+} tested against either PolyA/T and sshRNA templates. In the absence of DTT, Zn^{2+} has an IC_{50} of 0.6–1.7 μM when PolyA/T was used as template. With sshRNA, Zn^{2+} is ~7-fold less inhibitory. Presence or absence of 10 mM KCl did not significantly alter Zn^{2+} inhibition but presence of 4 mM DTT dramatically decreased the inhibitory activity of Zn^{2+} by 25–100-fold. This suppression of Zn^{2+} inhibitory activity by DTT is consistent with the ability of DTT to form very stable polymeric and monomeric coordination complexes with various metal ions using both of its sulfur donors (Kr zel et al., 2001).

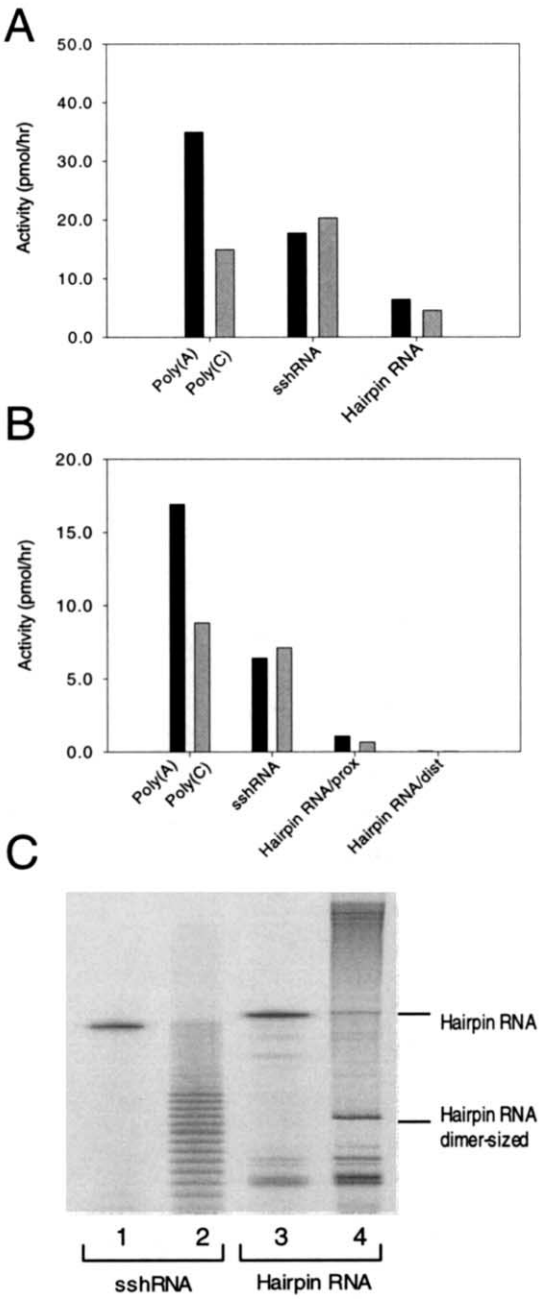

Fig. 4

4. Discussion

We have cloned the cDNA encoding the putative RdRp of HRV-16 and shown that the expressed protein is enzymatically active. HRV-16 3D polymerase is normally expressed as part of

Fig. 4. HRV16 3D polymerase activity on heteropolymeric templates. All the reactions contain one labeled nucleotide used at a concentration slightly above its K_m and three unlabeled nucleotides each at a concentration of 500 μM. Black bar, [α-^{33}P]-UTP labeled; grey bar, [α-^{33}P]-GTP labeled. (A) Radioactive incorporation as measured by TCA precipitation. Poly(A), poly(C) and sshRNA were all annealed to biotinylated DNA primers, whereas the reaction for the hairpin RNA does not contain primers. (B) Radioactive incorporation as measured by streptavidin capture on an NEN Flash Plate. All the RNAs were annealed to biotinylated DNA primers. For the hairpin RNA, two specific primers were tested, one proximal (prox) and the other distal (dist) to the putative self-priming site on the RNA. (C) Gel analysis of the reaction products using heteropolymeric RNA templates. The RNA samples were electrophoreses on a 5% acrylamide, 8 M urea gel. The starting RNA templates (lanes 1 and 3) were 3′ end-labeled with 5′-[^{32}P]pCp using T4 RNA ligase. The polymerase reactions were performed as in panel (A) with unlabeled templates and the reaction products were run (lanes 2 and 4).

Table 3
Kinetic analysis of HRV-16 3D polymerase[a]

Template	Substrate	K_m (μM)	k_{cat} (per h)	k_{cat}/K_m (per h per μM)
Poly(A)	UTP	12±1	833±38	72
Poly(C)	GTP	0.7±0.1	76±3	111
sshRNA	UTP	2.1±0.4	17.2±0.9	8
sshRNA	GTP	1.0±0.1	13.5±0.6	14
sshRNA	ATP	0.8±0.1	2.2±0.2	3
sshRNA	CTP	0.26±0.05	18.2±0.8	70

[a]The enzyme concentration used in the reaction was 0.02 μM. The reactions were done in the optimized buffer.

a viral polyprotein. Using a T7-based expression system, we were able to express high levels of this enzyme as an isolated polypeptide with a single additional methionine at the N-terminus and a 6His tag attached to the C-terminus by a glycine–serine spacer. Using this 6His tag, we purified the enzyme to near homogeneity by Ni-NTA affinity chromotography. The fact that we expressed an enzymatically active mature form of the 3D polymerase without co-expression of the 3C pro-

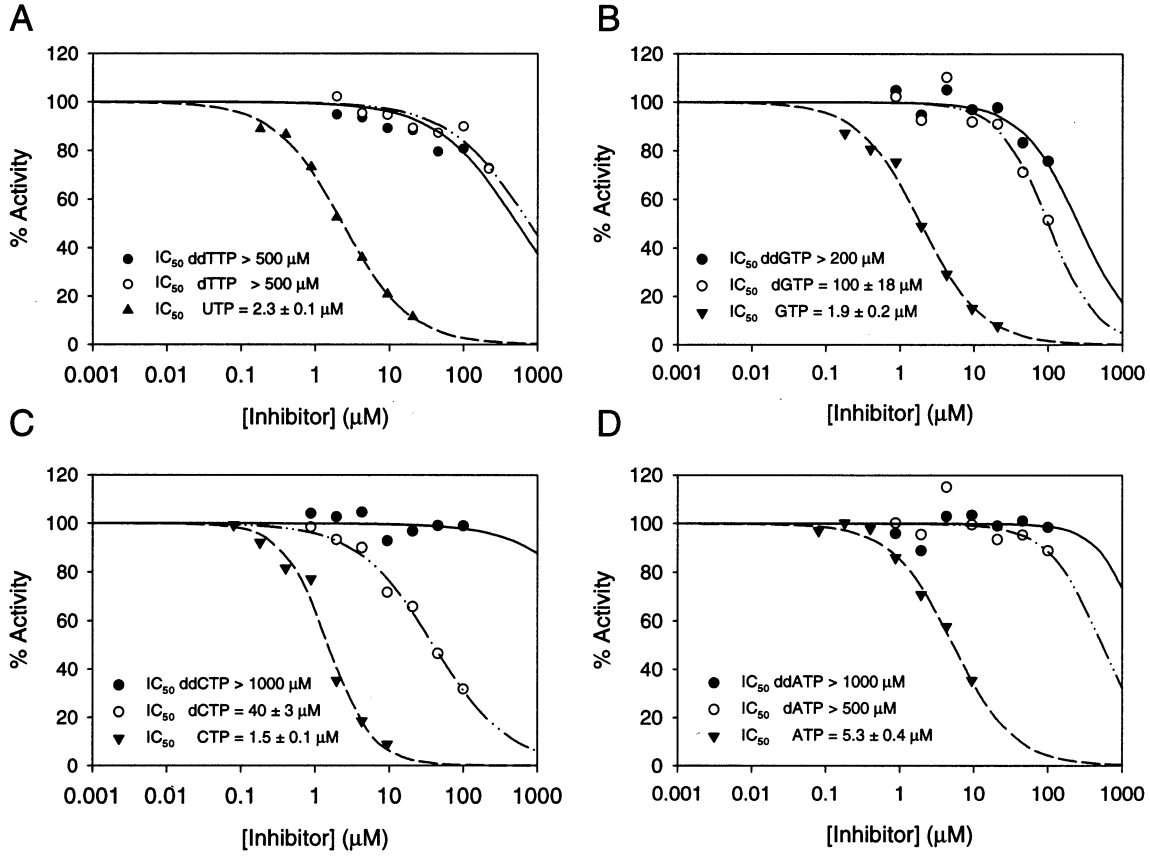

Fig. 5. Inhibition of HRV16 3D polymerase. The IC_{50} values were determined by non-linear regression using SIGMAPLOT 4.0. (A) Inhibition curves of UTP analogs. (B) Inhibition curves of GTP analogs. (C) Inhibition curves of CTP analogs. (D) Inhibition curves of ATP analogs.

Table 4
Inhibitory effect of Zn^{2+} ion[a]

Template	−KCl		+KCl	
	−DTT	+DTT	−DTT	+DTT
PolyA/T	0.6±0.3	63±4	1.7±0.4	46±6
sshRNA	4.0±0.6	100±10	12±1	100±19

[a]Reported in the table are the IC_{50} values of Zn^{2+} in μM. Mg^{2+} was present in all the reactions at 1.5 mM. When present, KCl and DTT were at 10 and 4 mM, respectively.

tease further supports the finding with both poliovirus (Plotch et al., 1989) and EMCV (Sankar and Porter, 1991) that picornaviral 3D polymerases do not need to be expressed as a fusion protein with the 3C protease for activity even though uncleaved 3CD is required for protease activity to process the viral capsid protein precursor, P1 (Burns et al., 1989). We showed that the observed polymerase activity did not result from a copurifying contaminant from *E. coli*, first by the absence of such activity in a similarly purified extract prepared from *E. coli* containing the empty vector, and second by the resistance of the observed polymerase activity to rifampicin, which is known to inhibit the *E. coli* DNA-dependent RNA polymerase (Chamberlin et al., 1983). Expression of active poliovirus 3D polymerase with an additional N-terminal methionine has been previously reported (Plotch et al., 1989) and the N-terminal methionine has been shown to be removed in *E. coli* (Hansen et al., 1997). Although we have not determined whether the N-terminal methionine of our rhinovirus 3D polymerase remains associated with the recombinant enzyme, it is conceivable that it is similarly removed. The C-terminal 6His tag did not seem to have impaired activity since both the 6His-tagged 3D polymerase and a partially purified preparation of HRV-16 3D polymerase without the tag had similar specific activity when assayed under the same conditions. The C-terminal 6His tag was also previously reported to have no deleterious effect on the activity of poliovirus 3D polymerase (Gohara et al., 1999).

HRV-16 3D polymerase was found to have varying preferences for different homopolymeric RNA templates, using poly(A) and poly(C) with high efficiency while exhibiting no activity on poly(G) and poly(U). This pattern of homopolymer specificity has been previously observed with HCV NS5B, another viral RdRp (Lohmann et al., 1997; Oh et al., 1999). While the polymerase activity of HRV-16 3D is primer-dependent for all four homopolymeric templates in the presence of Mg^{2+}, primer-independent de novo RNA synthesis or terminal transferase activity was promoted on poly(C) alone when Mg^{2+} was replaced with Mn^{2+}. This phenomenon was previously observed with poliovirus 3D polymerase (Arnold and Cameron, 1999). HRV-16 3D was capable of primer-independent synthesis on a heteropolymeric hairpin RNA using a copy-back mechanism previously reported for HCV NS5B (Behrens et al., 1996), forming a product of dimer size. The existence of secondary structure in heteropolymeric RNAs makes them prone to copy-back synthesis by self-priming which has been shown to compete efficiently with oligonucleotide-primed synthesis on the same heteropolymeric RNA (Behrens et al., 1996). We have confirmed this phenomenon by annealing biotinylated primers to the hairpin RNA template, enabling the products resulting from the exogenously primed synthesis to be captured on streptavidin-coated plates. Our use of a secondary-structureless heteropolymeric RNA (sshRNA) circumvented this self-priming problem and has enabled us to use a heteropolymeric RNA, in the Flash Plate format adaptable to high throughput screening, in much the same way as a linear homopolymeric RNA, but allowing all four ribonucleotides to be incorporated.

Rhinovirus-16 3D polymerase had a temperature optimum of 30 °C which is consistent with the optimum temperature of Rhinovirus growth of 33 °C (Gwaltney and Rueckert, 1997). The activity of HRV-16 3D polymerase was dependent on Mg^{2+}, and had an optimum Mg^{2+} concentration at 1.5 mM which is comparable to the 3 mM optimum for poliovirus and EMCV 3D polymerases (Neufeld et al., 1991a; Sankar and Porter, 1991). In the presence of Mn^{2+}, the 3D polymerase activity was increased by about 2-fold relative to that in the presence of Mg^{2+}. A 3- and 10-fold

higher stimulatory activity of Mn^{2+} relative to Mg^{2+} has also been observed for HCV NS5B polymerase (Ferrari et al., 1999) and poliovirus 3D polymerase (Arnold et al., 1999), respectively. Because Mn^{2+} promotes misincorporation of dNTPs, ddNTPs and non-complementary NTPs by poliovirus 3D polymerase (Arnold et al., 1999), we studied the substrate specificity of HRV-16 3D polymerase in the presence of either Mg^{2+} or Mn^{2+} using poly(A) as template. In the presence Mg^{2+}, HRV-16 3D was accurate in the utilization of only NTPs complementary to the template and had no reverse transcriptase activity. However, in presence of a 100-fold molar excess of UTP to [^{33}P]-dTTP, the HRV-16 3D polymerase was able to misincorporate a low level of [^{33}P]-dTMP. This suggests that while continuous DNA synthesis by reverse transcription was not possible in the presence Mg^{2+}, the enzyme can intermittently misincorporate a low level of deoxynucleotides during RNA synthesis. Unlike poliovirus 3D polymerase, replacement of Mg^{2+} by Mn^{2+} did not affect the base specificity of HRV-16 3D, but severely compromised the ability of the enzyme to discriminate the sugar moiety of the nucleotide substrates.

The K_m and k_{cat} values determined for UTP using poly(A) as template were within 4-fold of the corresponding parameters previously described for poliovirus 3D polymerase (Neufeld et al., 1991b; Arnold and Cameron, 1999). The higher efficiency of the poly(A) template as compared with poly(C) was mainly manifested in the turnover rate of the nucleotide substrate where the k_{cat} for UTP was about 11-fold greater than the k_{cat} for GTP. This suggests that the polymerase molecule may be more processive on the poly(A) template compared with the poly(C) template. On the other hand, the K_m for GTP is 17-fold lower than that of UTP, suggesting that the number of hydrogen bonds involved in base pairing with the complementary nucleotide on the template may also contribute to binding of the nucleotide substrate to the polymerase complex. When the heteropolymeric sshRNA was used as template, the turn over rate for all four nucleotides became more comparable to each other but with a mean k_{cat} 35-fold lower than the mean k_{cat} for UTP and GTP determined for the homopolymeric templates. This is consistent with the sshRNA being a template of intermediate efficiency relative to the efficiency extremes observed for the four homopolymeric templates. The K_m for UTP was also decreased by about 6-fold using the heteropolymeric template, suggesting that the polymerase complex formed on heteropolymeric RNA may adopt a more optimal conformation with increased affinity to certain nucleotide substrates. These findings on the K_m and k_{cat} of nucleotide substrates on homopolymeric and heteropolymeric templates are consistent with a previous observation using HCV NS5B polymerase (Lohmann et al., 1998).

Three types of zinc binding sites are known to exist in proteins: catalytic binding sites found in zinc metalloenzymes such as horse liver alcohol dehydrogenase (Ramaswamy et al., 1994), structural binding sites examplified by HCV protease (Kim et al., 1996) and HIV integrase (Esposito and Craigie, 1999) and inhibitory binding sites in enzymes that do not contain zinc, such as aldehyde dehydrogenase (Maret et al., 1999). Rhinovirus 3D polymerase is probably not a zinc containing enzyme with catalytic or structural zinc binding sites, as zinc was not reported in the crystal structure of the closely related poliovirus 3D polymerase (Hansen et al., 1997). However, given the ability of zinc to inhibit the activity of rhinovirus 3D polymerase, the presence of an inhibitory binding site for zinc in rhinovirus 3D polymerase is a possibility. It is not clear at this point whether susceptibility to zinc is specific to rhinovirus polymerase or whether it applies to related viral RdRps as well. The inhibition of rhinovirus 3D polymerase by zinc, observed in this study, is not likely due to displacement of the catalytically essential Mg^{2+} ion, because the Mg^{2+} optimum is at 1.5 mM while the IC_{50} of Zn^{2+} is 12 μM. Several potential mechanisms have been proposed for the observed inhibition of rhinovirus replication in vitro by zinc (Korant et al., 1974; Korant and Butterworth, 1976; Novick et al., 1996). Inhibition of the 3D polymerase could constitute an additional mechanism whereby zinc exerts its putative antiviral effect on rhinoviruses. Zinc has been reported to be efficacious

for the treatment of rhinovirus-associated cold symptoms, but these results are controversial (Godfrey et al., 1996; Hirt et al., 2000; Turner, 2001).

Using purified recombinant HRV-16 3D polymerase and a secondary-structureless heteropolymeric RNA (sshRNA) we have developed a highly sensitive and quantitative Flash Plate assay to characterize the activity of this RdRp. The assay is adaptable to high throughput screening of compounds that inhibit the 3D polymerase and is a first step toward a more systematic structure–activity study of the enzyme as a target for antiviral therapy.

References

Andrews, N.C., Levin, D., Baltimore, D., 1985. Poliovirus replicase stimulation by terminal uridylyl transferase. J. Biol. Chem. 260, 7628–7635.

Arnold, J.J., Cameron, C.E., 1999. Poliovirus RNA-dependent RNA polymerase ($3D^{pol}$) is sufficient for template switching in vivo. J. Biol. Chem. 274, 2706–2716.

Arnold, J.J., Ghosh, S.K.B., Cameron, C.E., 1999. Poliovirus RNA-dependent RNA polymerase ($3D^{pol}$): divalent cation modulation of primer, template, and nucleotide selection. J. Biol. Chem. 274, 37060–37069.

Behrens, S.-E., Tomei, L., De Francesco, R., 1996. Identification and properties of the RNA-dependent RNA polymerase of hepatitis C virus. EMBO J. 15, 12–22.

Bruenn, J.A., 1991. Relationships among the positive-strand and double-strand RNA viruses as viewed through their RNA-dependent RNA polymerases. Nucleic Acids Res. 19, 217–226.

Burns, C.C., Lawson, M.A., Semler, B.L., Ehrenfeld, E., 1989. Effects of mutations in poliovirus 3Dpol on RNA polymerase activity and on polyprotein cleavage. J. Virol. 63, 4866–4874.

Bush, R.K., Busse, W.W., Flaherty, D., Warshauer, D., Dick, E.C., Reed, C.E., 1978. Effects of experimental rhinovirus 16 infection on airways and leukocyte function in normal subjects. J. Allergy Clin. Immunol. 61, 80–87.

Calhoun, W.J., Swenson, C.A., Dick, E.C., Schwartz, L.B., Lemanske, R.F., Jr, Busse, W.W., 1991. Experimental rhinovirus 16 infection potentiates histamine release after antigen bronchoprovocation in allergic subjects. Am. Rev. Respir. Dis. 144, 1267–1273.

Chamberlin, M., Kingston, R., Gilman, M., Wiggs, J., de Vera, A., 1983. Isolation of bacterial and bacteriophage RNA polymerases and their use in synthesis of RNA in vitro. Methods Enzymol. 101, 540–568.

Couch, R.B., 1990. Rhinoviruses. In: Fields, B.N., Knipe, D.M., Chanock, R.M., Hirsch, M.S., Jmelnick, L., Monath, T.P., Roizman, B. (Eds.), Virology. Raven Press, New York, pp. 607–629.

Duechler, M., Skern, T., Sommergruber, W., Neubauer, C., Gruendler, P., Fogy, I., Blaas, D., Kuechler, E., 1987. Evolutionary relationships within the human rhinovirus genus: comparison of serotypes 89, 2 and 14. Proc. Natl. Acad. Sci. USA 84, 2605–2609.

Esposito, D., Craigie, R., 1999. HIV integrase structure and function. Adv. Virus Res. 52, 319–333.

Ferrari, E., Wright-Minogue, J., Fang, J.W.S., Baroudy, B.M., Lau, J.Y.N., Hong, Z., 1999. Characterization of soluble hepatitis C virus RNA-dependent RNA polymerase expressed in *Escherichia coli*. J. Virol. 73, 1649–1654.

Gerber, K., Wimmer, E., Paul, A.V., 2001. Biochemical and genetic studies of the initiation of human rhinovirus two RNA replication: Purification and enzymatic analysis of the RNA-dependent RNA polymerase $3D^{pol}$. J. Virol. 75, 10969–10978.

Godfrey, J.C., Godfrey, N.J., Novick, S.G., 1996. Zinc for treating the common cold: review of all clinical trials since 1984. Altern. Ther. Health Med. 2, 63–72.

Gohara, D.W., Ha, C.S., Kumar, S., Ghosh, B., Arnold, J.J., Wisniewski, T.J., Cameron, C.E., 1999. Production of 'authentic' poliovirus RNA-dependent RNA polymerase ($3D^{pol}$) by ubiquitin-protease-mediated cleavage in *Escherichia coli*. Protein Exp. Purif. 17, 128–138.

Greve, J.M., Davis, G., Meyer, A.M., Forte, C.P., Yost, S.C., Marlor, C.W., Kamarck, M.E., McClelland, A., 1989. The major human rhinovirus receptor is ICAM-1. Cell 56, 839–847.

Gwaltney, J., Jr, Rueckert, R.R., 1997. Rhinovirus. In: Richman, D.D., Whitley, R.J., Hayden, F.G. (Eds.), Clinical Virology. Churchill Livingstone, New York, pp. 1025–1047.

Hansen, J.L., Long, A.M., Schultz, S.C., 1997. Structure of the RNA-dependent RNA polymerase of poliovirus. Structure 5, 1109–1122.

Hirt, M., Nobel, S., Barron, E., 2000. Zinc nasal gel for the treatment of common cold symptoms: a double-blind, placebo-controlled trial. Ear Nose Throat J. 79, 778–782.

Hofer, F., Gruenberger, M., Kowalski, H., Machat, H., Huettinger, M., Kuechler, E., Blass, D., 1994. Members of the low density lipoprotein receptor family mediate cell entry of a minor-group common cold virus. Proc. Natl. Acad. Sci. USA 91, 1839–1842.

Hughes, P.J., North, C., Jellis, C.H., Minor, P.D., Stanway, G., 1988. The nucleotide sequence of human rhinovirus 1B: molecular relationships within the rhinovirus genus. J. Gen. Virol. 69, 49–58.

Kim, J.L., Morgenstern, K.A., Lin, C., Fox, T., Dwyer, M.D., Landro, J.A., Chambers, S.P., Markland, W., Lepre, C.A., O'Malley, E.T., Harbeson, S.L., Rice, C.M., Murcko, M.A., Caron, P.R., Thomson, J.A., 1996. Crystal structure of the hepatitis C virus NS3 protease domain complexed with a synthetic NS4A cofactor peptide. Cell 87, 343–355.

Korant, B.D., Butterworth, B.E., 1976. Inhibition by zinc of rhinovirus cleavage: interaction of zinc with capsid polypeptides. J. Virol. 18, 298–306.

Korant, B.D., Kauer, J.C., Butterworth, B.E., 1974. Zinc ions inhibit replication of rhinoviruses. Nature 248, 588–590.

Koonin, E.V., 1991. The phylogeny of RNA-dependent RNA polymerases of positive-strand RNA viruses. J. Gen. Virol. 72, 2197–2206.

Kr zel, A., Lesniak, W., Jezowska-Bojczuk, M., Mlynarz, P., Brasum, J., Kozlowski, H., Bal, W., 2001. Coordination of heavy metals by dithiothreitol, a commonly used thiol group protectant. J. Inorg. Biochem. 84, 77–88.

Kuhn, R.J., Wimmer, E., 1987. The replication of picornaviruses. In: Rowlands, D.J., Mahy, B.W.J., Mayo, M. (Eds.), The Molecular Biology of Positive Strand RNA Viruses. Academic Press, New York, pp. 17–51.

Lee, W.-M., Wang, W., Rueckert, R.R., 1994. Complete sequence of the RNA genome of human rhinovirus 16, a clinically useful common cold virus belonging to the ICAM-1 receptor group. Virus Genes 9, 177–181.

Lemanske, R.F., Jr, Dick, E.C., Swenson, C.A., Vrtis, R.F., Busse, W.W., 1989. Rhinovirus upper respiratory infection increases airway hyperreactivity and late asthmatic reactions. J. Clin. Invest. 83, 1–10.

Lohmann, V., Körner, F., Herian, U., Bartenschlager, R., 1997. Biochemical properties of hepatitis C virus NS5B RNA-dependent RNA polymerase and identification of amino acid sequence motifs essential for enzymatic activity. J. Virol. 71, 8416–8428.

Lohmann, V., Roos, A., Körner, F., Koch, J.O., Bartenschlager, R., 1998. Biochemical and kinetic analyses of NS5B RNA-dependent RNA polymerase of the hepatitis C virus. Virology 249, 108–118.

Lubinski, J.M., Ransone, L.J., Dasgupta, A., 1987. Primer-dependent synthesis of covalently linked dimeric RNA molecules by poliovirus replicase. J. Virol. 61, 2997–3003.

Maret, W., Jacob, C., Valee, B.L., Fischer, E.H., 1999. Inhibitory sites in enzymes: zinc removal and reactivation by thionein. Proc. Natl. Acad. Sci. USA 96, 1936–1940.

Mathews, D.H., Sabina, J., Zuker, M., Turner, D.H., 1999. Expanded sequence dependence of thermodynamic parameters improves prediction of RNA secondary structure. J. Mol. Biol. 288, 911–940.

Morrow, C.D., Lubinski, J., Hocko, J., Gibbons, G.F., Dasgupta, A., 1985. Purification of a soluble template-dependent rhinovirus RNA polymerase and its dependence on a host cell protein for viral RNA synthesis. J. Virol. 53, 266–272.

Morrow, C.D., Warren, B., Lentz, M.R., 1987. Expression of enzymatically active poliovirus RNA-dependent RNA polymerase in *Escherichia coli*. Proc. Natl. Sci. USA 84, 6050–6054.

Neufeld, K.L., Richards, O.C., Ehrenfeld, E., 1991a. Expression and characterization of poliovirus proteins $3B^{VPg}$, $3C^{pro}$, and $3D^{pol}$ in recombinant baculovirus-infected Spodoptera frugiperda cells. Virus Res. 19, 173–188.

Neufeld, K.L., Richards, O.C., Ehrenfeld, E., 1991b. Purification, characterization, and comparison of poliovirus RNA polymerase from native and recombinant sources. J. Biol. Chem. 266, 24212–24219.

Novick, S.G., Godfrey, J.C., Wilder, H.R., Godfrey, N.J., 1996. How does zinc modify the common cold. Med. Hypotheses 46, 295–302.

Oh, J.-W., Ito, T., Lai, M.M.C., 1999. A recombinant hepatitis C virus RNA-dependent RNA polymerase capable of copying the full-length viral RNA. J. Virol. 73, 7694–7702.

Oliveira, M.A., Zhao, R., Lee, W.-M., Kremer, M.J., Minor, I., Ruechert, R.R., Diana, G.D., Pevear, D.C., Dutko, F.J., McKinlay, M.A., Rossmann, M.G., 1993. The structure of human rhinovirus 16. Structure 1, 51–68.

Palmenberg, A.C., 1990. Proteolytic processing of picornaviral polyprotein. Annu. Rev. Microbiol. 44, 603–623.

Patick, A.K., Potts, K.E., 1998. Protease inhibitors as antiviral agents. Clin. Microbiol. Rev. 11, 614–627.

Pitkaranta, A., Hayden, F.G., 1998. Rhinoviruses: important respiratory pathogens. Ann. Med. 30, 529–537.

Plotch, S.J., Palant, O., Gluzman, Y., 1989. Purification and properties of poliovirus RNA polymerase expressed in *Escherichia coli*. J. Virol. 63, 216–225.

Poch, O., Sauvaget, I., Delarue, M., Tordo, N., 1989. Identification of four conserved motifs among the RNA-dependent polymerase encoding elements. EMBO J. 8, 3867–3874.

Porter, A.G., 1993. Picornaviral nonstructural proteins: emerging roles in virus replication and inhibition of host functions. J. Virol. 67, 6917–6921.

Racaniello, V.R., Baltimore, D., 1981. Molecular cloning of poliovirus cDNA and determination of the complete nucleotide sequence of the viral genome. Proc. Natl. Acad. Sci. USA 78, 4887–4891.

Ramaswamy, S., Eklund, H., Plapp, B.V., 1994. Structure of horse liver alcohol dehydrogenase complexed with NAD+ and substituted benzyl alcohols. Biochemistry 33, 5230–5237.

Richards, O.C., Ehrenfeld, E., 1990. Poliovirus RNA replication. Curr. Top. Microbiol. Immunol. 161, 89–119.

Richards, O.C., Ivanoff, L.A., Bienkowska-Szewczyk, K., Butt, B., Petteway, S.R., Rothstein, M.A., Ehrenfeld, E., 1987. Formation of poliovirus RNA polymerase 3D in *Escherichia coli* by cleavage of fusion protein expressed from cloned viral cDNA. Virology 161, 348–356.

Rodriguez, P.L., Carrasco, L., 1992. Gliotoxin: Inhibitor of poliovirus RNA synthesis that blocks the viral RNA polymerase 3Dpol. J. Virol. 66, 1971–1976.

Rothstein, M.A., Richards, O.C., Amin, C., Ehrenfeld, E., 1988. Enzymatic activity of poliovirus RNA polymerase synthesized in *Escherichia coli* from viral cDNA. Virology 164, 301–308.

Sankar, S., Porter, A.G., 1991. Expression, purification, and properties of recombinant encephalomyocarditis virus RNA-dependent RNA polymerase. J. Virol. 65, 2993–3000.

Semler, B.L., Kuhn, R.J., Wimmer, E., 1988. Replication of the poliovirus genome. In: Domingo, E., Holland, J.J., Ahl-

quist, P. (Eds.), RNA Genetics. CRC Press, Boca Raton, Florida, pp. 23–48.

Skern, T., Sommergruber, W., Blaas, D., Gruendler, P., Fraundorfer, F., Pieler, C., Fogy, I., Kuechler, E., 1985. Human rhinovirus 2: complete nucleotide sequence and proteolytic processing signals in the capsid protein region. Nucleic Acids Res. 13, 2111–2126.

Stanway, G., Hughes, P.J., Mountford, R.C., Minor, P.D., Almond, J.W., 1984. The complete nucleotide sequence of a common cold virus: human rhinovirus 14. Nucleic Acids Res. 12, 7859–7875.

Tomassini, J.E., Colonno, R.J., 1986. Isolation of a receptor protein involved in attachment of human rhinoviruses. J. Virol. 58, 290–295.

Turner, R.B., 2001. Ineffectiveness of intranasal zinc gluconate for prevention of experimental rhinovirus colds. Clin. Infect. Dis. 33, 1865–1870.

Van Dyke, T.A., Flanegan, J.B., 1980. Identification of poliovirus polypeptide P63 as a soluble RNA-dependent RNA polymerase. J. Virol. 35, 732–740.

Wang, Q.M., 1999. Protease inhibitors as potential antiviral agents for the treatment of picornaviral infections. Prog. Drug Res. 52, 197–219.

Young, D.C., Tuschall, D.M., Flanegan, J.B., 1985. Poliovirus RNA-dependent RNA polymerase and host cell protein synthesized product RNA twice the size of poliovirion RNA in vitro. J. Virol. 54, 256–264.